ACS OMEGA

Open Access

http://pubs.acs.org/journal/acsodf

Review

Unveiling the Molecular Secrets: A Comprehensive Review of Raman Spectroscopy in Biological Research

Anshuman Chandra, Vimal Kumar, Umesh Chandra Garnaik, Rima Dada, Imteyaz Qamar, Vijay Kumar Goel, and Shilpi Agarwal*

Cite This: *ACS Omega* 2024, 9, 50049−50063

Read Online

ACCESS | Metrics & More | Article Recommendations | Supporting Information

ABSTRACT: Raman spectroscopy has been proven to be a fast, convenient, and nondestructive technique for advancing our understanding of biological systems. The Raman effect originates from the inelastic scattering of light which directly probe vibration/rotational states in biological molecules and materials. Despite numerous advantages over infrared spectroscopy and continuous technical as well as operational improvement in Raman spectroscopy, an advanced development of the device and more applications have become possible. In this review, we explore the principles, techniques, and myriad applications of Raman spectroscopy in the realm of biology. We begin by providing an overview of Raman spectroscopy, highlighting its significance in unraveling the complexities of biological research. The focus of this review is on Raman spectroscopy concepts and methods, clarifying the fundamentals of Raman scattering and spectral interpretation. The review also highlights the key experimental considerations for productive biological applications. We explore the broad range of Raman applications including molecular structure, biomolecular composition, disease detection, and medication discovery. The Raman imaging and mapping can also be used to visualize biological samples at the molecular level. Raman spectroscopy is still developing, giving fresh insights and remedies, from biosensing to its use in tissue engineering and regenerative medicine. This review sheds light on the past, present, and future of Raman spectroscopy; it also highlights promising directions of future research developments and serves as a thorough resource for all researchers.

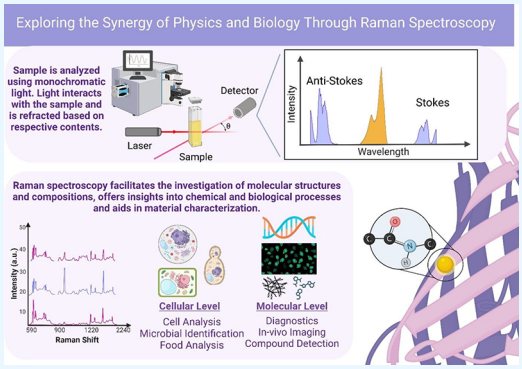

1. INTRODUCTION

1.1. Overview of Raman Spectroscopy. In order to determine the vibrational modes of molecules, scientists employ the spectroscopic technique known as Raman spectroscopy, which bears the name of the Indian physicist C.V. Raman.[1] Chemistry routinely uses Raman spectroscopy to give molecules a distinctive structural fingerprint. The foundation of Raman spectroscopy is Raman scattering, commonly referred to as inelastic photon scattering. Lasers in the visible, near-infrared, or near-ultraviolet spectrum, as well as X-rays, are widely employed to produce monochromatic light. The energy of the laser photons is pushed up or down by interactions of the laser light with phonons, molecular vibrations, or other excitations in the system. The energy shift reveals information about the vibrational modes of the system, in which a laser beam is typically used to illuminate a sample and an objective lens collects the electromagnetic radiation emitted by the lit area and directs it toward a monochromator. The elimination of elastically scattered light at the laser line's wavelength through the use of a notch filter, edge pass filter, or band-pass filter is known as Rayleigh scattering. Separating the strongly Rayleigh scattered laser light from the weakly inelastically scattered light a process known as "laser rejection" was for a long time the main challenge in obtaining Raman spectra. Spontaneous Raman scattering is frequently quite faint. In the past, holographic gratings and several dispersion stages were utilized in Raman spectrometers to create a high level of laser rejection. For dispersive Raman setups in the past, photomultipliers were the detector of choice, which led to lengthy acquisition periods. However, current technology nearly invariably contains notch or edge filters to stop lasers. The most common types dispersive single-stage spectrographs used with NIR lasers are axial transmissive (AT) or Czerny-Turner (CT) monochromators coupled with CCD detectors; however, Fourier transform (FT) spectrometers are also often employed. When "Raman spectroscopy" is mentioned, it typically refers to vibrational Raman using laser wavelengths that are not absorbed by the substance.

Received: January 18, 2024
Revised: May 30, 2024
Accepted: June 5, 2024
Published: December 3, 2024

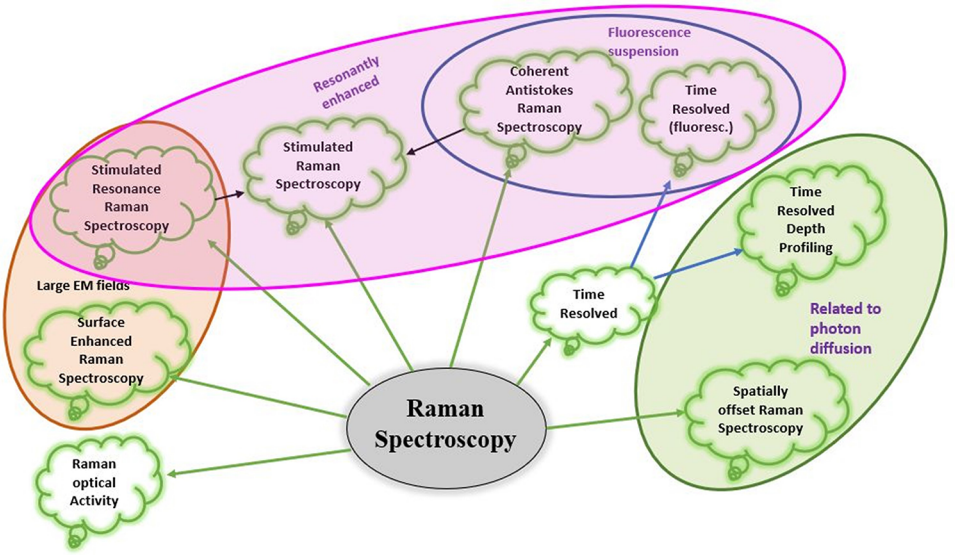

Figure 1. Raman spectroscopy and its variant.

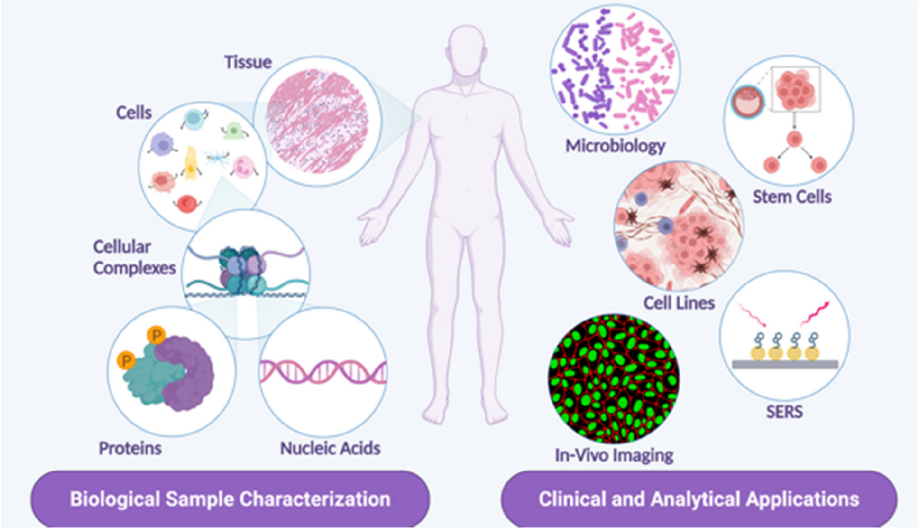

Figure 2. Potential biological applications of Raman spectroscopy. (Created with BioRender.com.)

Among the numerous types of Raman spectroscopy are surface-enhanced Raman, resonance Raman, tip-enhanced Raman, polarized Raman, Coherent Raman, transmission Raman, spatially offset Raman, and hyper Raman. Figure 1 shows all the promising variants of Raman spectroscopy. The inelastic scattering of light was predicted by Adolf Smekal in 1923, but it was not discovered until 1928.[2] The Raman effect was first observed in inorganic crystals in 1928 by the Indian scientists C. V. Raman and K. S. Krishnan[3] and separately by Grigory Landsberg and Leonid Mandelstam. In 1930, Raman won the Physics Nobel Prize for making this discovery. In 1929, Franco Rasetti made the first observation of Raman spectra in gases.[3] Between 1930 and 1934, Czechoslovak physicist George Placzek developed a complete, ground-breaking theory of the Raman phenomenon.[4] The primary source of illumination, initially for photography and later for spectrophotometric detection, was the mercury arc. Raman spectroscopy was used to compile the first database of molecular vibrational frequencies in the years after its discovery.

There are many applications of Raman spectroscopy that can be applied to biological studies. Biomolecules are vital components of life. They are essential to all life processes, performing critical metabolic reactions and regulating a live organism's general biochemistry. A variety of macromolecules, including nucleic acids, proteins, lipids, and carbohydrates, play a role in maintaining cellular functional homeostasis. Any biological substance (cell, tissue, etc.) is composed of a variety of biomolecules. As a result, it is critical to understand the structure and characteristics of each biomolecule individually. Interestingly, each of these biomolecules has a separate chemical identity and hence unique molecular structures. Consequently, these biomolecules create a characteristic Raman spectrum.[5,6] Raman spectroscopy is used for identifying biological fluids, including blood, saliva, urine, perspiration, vaginal fluid, and menstrual blood. These are often seen in situations involving various crimes. The investigation of body fluids aids in determining a probable relationship between the suspect, crime, and victim. Body fluids may be used to extract a DNA profile, which can then be used to identify and

https://doi.org/10.1021/acsomega.4c00591
ACS Omega 2024, 9, 50049−50063

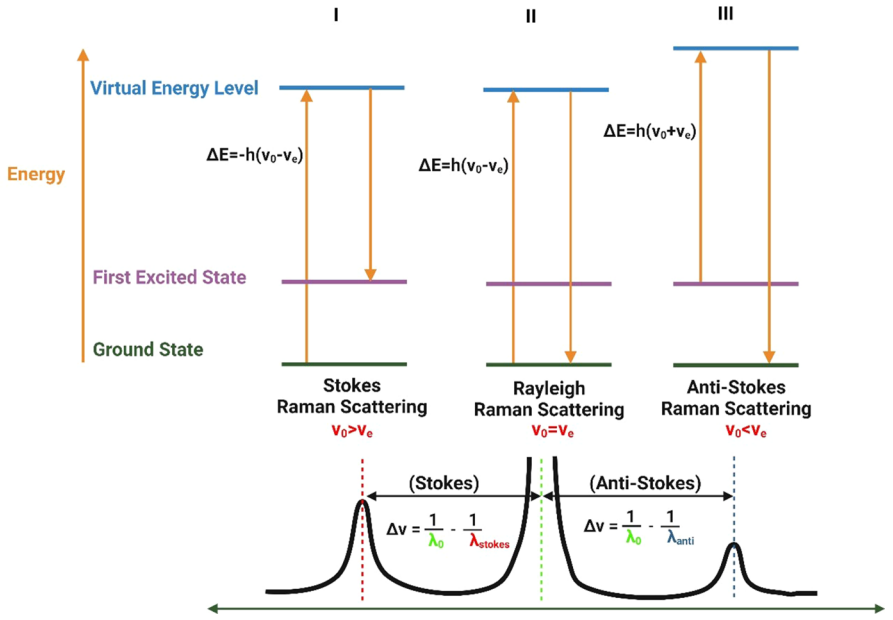

Figure 3. Raman scattering process and spectral information. (Created with BioRender.com.)

personalize someone. Sikirzhytskaya's team[7,8] has proved the effectiveness of Raman spectroscopy for the investigation of numerous bodily fluids, and other researchers have expanded this work.

The pathophysiology of many neurodegenerative illnesses is not well understood. The scarcity of viable biomarkers and disease prevention methods[9,10] necessitates the development of novel approaches for efficiently probing disease processes and detecting early biomarkers predictive of illness onset. Raman spectroscopy is an established technique for label-free fingerprinting and imaging of molecules based on their chemical composition and structure. While Raman spectroscopy has long been used in the chemical community to analyze isolated biological molecules, its use in the research of therapeutically relevant biological species, disease cause, and diagnostics has increased dramatically over the past decade.[11−16] The rising number of biological applications has demonstrated Raman spectroscopy's potential for detecting new biomarkers, allowing for quick and reliable screening of disease susceptibility and onset.[17−19] Figure 2 shows the potential biological applications of Raman spectroscopy covered in the review.

1.2. Significance of Raman Spectroscopy in Biological Research. This work aims to build a database of molecular fingerprints that aids in defining the chemical structure of biological tissues by including the bulk of the conspicuous peaks observed in natural tissues. The definition of peaks in the same regions of the Raman spectrum are defined in relatively comparable ways despite the employment of a variety of approaches. The quantity and quality of data relevant to Raman spectra and their findings have significantly improved as a result of the development of a unique collection of frequencies utilized in Raman spectroscopy study. This review provides a brief database on the main Raman lines for researchers who want to utilize Raman spectroscopy to examine natural tissues. Additionally, this is of great use to individuals whose line of work entails examining cancerous tissues utilizing Raman analysis. It is a method that is frequently used to identify biological tissues. This method is chosen by scientists to ascertain the chemical and structural properties of synthetic and natural tissues. Using the peak frequencies at 1300 cm^{-1} (CH_2 twist), 1440 cm^{-1} (CH_2 bend), 1656 cm^{-1} (C═C), and the lipid constituents and chemical structures are well analyzed. Peak frequencies at 1300 cm^{-1} (CH_2 bend), 1440 cm^{-1} (CH_2), and 1656 cm^{-1} (amide I) are useful for exploring protein concentrations.[20] The modifications brought on by cell proliferation can be monitored using Raman spectroscopy. In order to do this, cultures are examined throughout both their nonproliferative and proliferative growth phases. After that, the relative concentrations of biological components such as RNA, DNA, proteins, and lipids in cell nuclei and membranes are estimated. Reproducible differences are identified and assessed using the relative amounts and ratios of biological components. This information can be helpful for in vivo cancer cell populations that are actively multiplying detection can be done via Raman analysis.[21]

Koljenović and his team used Raman microscopy to analyse meningioma and normal dura mater in order to see if it would be able to develop an in vivo Raman technique for the regulation of meningioma reactions. Raman maps were produced using cryosections of the dura and meningiomas from 20 patients. Maps and histology were compared to identify the Raman spectra as either meningioma or dura. There are more variances between them as a result of the dura's high collagen content and meningiomas' increased lipid content. On the basis of a linear discriminant analysis of Raman spectra, the classification model for dura and meningioma demonstrated 100% accuracy.[22] The meningioma and dura can be separated from one another using Raman spectra. Raman spectroscopy is therefore a formidable rival for the management of meningioma surgery. Jalkanen and his team analyzed the structures of DNA and proteins using vibrational spectroscopy. In addition, the research of biomolecule hydration and binding integrated experimental and theoretical approaches. Peptides and amino acids made up the vast majority of the substances that were meticulously examined. The objective was to fully comprehend the

https://doi.org/10.1021/acsomega.4c00591
ACS Omega 2024, 9, 50049−50063

experimentally determined vibrational spectra of the molecules and to ascertain the function, structure, and electronic properties of the molecules in the various environments. As more environmental and biophysical tests employ spectroscopic methods, a more thorough understanding of the phenomenon from a sound theoretical foundation is required.[23]

2. PRINCIPLES AND TECHNIQUES OF RAMAN SPECTROSCOPY

2.1. Raman Scattering and Spectral Interpretation. Raman scattering is a type of inelastic scattering by which photons are scattered by matter, resulting in both an energy exchange and a change in light direction. Technically scattering occurs when a strong light source, often laser impacts a sample, the amount of light scattered from the laser is in numerous directions. Most of the scattered light has the same wavelength of the light that comes in, but only a small proportion of it may reach the sample and indicate a small amount of energy. Changes in frequency and wavelength can be used to identify energy shifts in scattered light.

To assess the physical and chemical composition of a sample, Raman spectroscopy employs the following scattering mechanism: Rayleigh scattering, Stokes scattering, and anti-Stokes scattering. Figure 3 shows the Raman scattering process and spectral information.

Here ΔE represents the photon energy difference between the virtual energy state and ground energy state. ν_o is the incident Raman frequency, whereas ν_e defines scattered Raman frequency. $\Delta\nu$ gives the Raman shift in cm^{-1}. I: Energy is absorbed by atoms or molecule. A scattered photon's energy is less than that of an incoming photon. Vibrational energy is gained by the atom or molecule. II: Here there is no exchange of energy. The incident and scattered photons have the same energy. Frequency shifts are symmetric. III: The energy is lost by an atom or molecule. The energy of the incident photon is smaller than that of the scattered photon.

Raman Scattering light wavelength is determined by the wavelength of the excited light. As a result of comparing spectra obtained with various lasers, the Raman scatter wavelength is an incorrect value. Hence the position of the Raman scatter is away from the excitation wavelength converted into a Raman shift:

$$\Delta\nu(\mathrm{cm}^{-1}) = \left(\frac{1}{\lambda_0(\mathrm{nm})} - \frac{1}{\lambda_1(\mathrm{nm})}\right)^{*} \frac{(10^7\ \mathrm{nm})}{(\mathrm{cm})}$$

Here the first term represents the wavenumber Raman shift in cm^{-1} and λ_0 and λ_1 define the wavelength of the excitation laser and Raman scatter in nanometers, respectively.

In most cases, Raman spectra are plotted with the intensity or number of counts on the y-axis and the Raman Shift frequency along the x-axis. Raman shift is defined as the frequency difference between the laser light and the scattered or dispersed light. Here the Raman shift is not related to the wavelength of the laser and is given in wavenumbers. The number of events measured by the spectrometer per second for a certain Raman shift is proportional to the amount of light detected defining the count rate. Searching for molecular functional groups, which are different molecule components, is the first approach of analyzing Raman spectra. Raman spectra depict functional group vibrations at discrete Raman shifts. These structural changes enable an unknown molecule to be related to a known class of compounds. The complete analysis of Raman spectra depends on symmetry, polarization, and selection rules. Observing the polarization of scattered photons can help us understand the relationship between Raman activity and molecular symmetry, which can aid in the assignment of peaks in Raman spectra. Only specific Raman-active modes are accessible with polarized light in a single direction. Changing the polarization, on the other hand, enables access to alternative modes. Each mode is classified based on its symmetry. Except when phonon confinement is evident, according to a selection criterion applicable exclusively to ordered solid materials, exclusively phonons with zero phase angle may be observed by IR and Raman.

The Raman shifts and relative intensities of the material's spectra can identify the material using Raman bands. With individual band modifications, a band's intensity may shift, narrow, or broaden, or shift in intensity. These changes can provide details about the sample's stresses, crystallinity variations, and material amount. Differences in spectra with sample position will reveal differences in the uniformity of the material. The frequencies of vibration are determined by the masses of the atoms engaged and the strength of their connections. Raman shifts are small in the case of heavy atoms and weak links. Raman shifts are large in light atoms and strong bonds. Once we identify the Raman shifts, we can plot them to get the Raman spectra. Each Raman peak corresponds to a certain frequency of light absorbed by the sample, resulting in vibration. The Raman spectrum allows us to identify and evaluate a wide range of chemicals since these frequencies come under the chemical fingerprint region. For example, we know that two carbon atoms with a double bond vibrate around 1300 cm^{-1} and the C−C weaker single bond at 800 cm^{-1}. When we beam our green laser on the molecules, they absorb the light frequencies that we detect on the Raman spectrum. The C═C peak will be about 1650 cm^{-1}, and the C−C peak will be around 800 cm^{-1}. This implies that Raman spectroscopy can easily distinguish between these two types of bonding as well as molecules.

2.2. Instrumentation and Experimental Setup. Raman spectroscopy was named after its creator, C.V. Raman, who published the first article on the technique alongside K.S. Krishnan.[24] Raman spectroscopy provides a flexible C═C technique for analyzing several sorts of forensic evidence. It solves most existing spectroscopic technique constraints and provides qualitative as well as quantitative data about the material under investigation. In qualitative analysis, the frequency of scattered radiation is assessed, whereas quantitative analysis measures the intensity of scattered radiation.[25,26] Raman and Krishnan used a mercury lamp and photographic plates to capture spectra. Due to limited light sources, detector sensitivity, and the low Raman scattering cross sections of most materials, early spectra took hours or even days to acquire.[24] Technological advances in recent times improves the quality of components used in the Raman spectroscopic techniques. Raman spectrometer is made up of many basic components, including a laser that acts as an excitation source to cause Raman scattering. Solid state lasers are commonly employed in current Raman equipment, with popular wavelengths including 532, 785, 830, and 1064 nm. Shorter wavelength lasers offer higher Raman scattering cross sections, resulting in a stronger signal; nevertheless, the incidence of fluorescence increases with shorter wavelength. Because of this, many Raman systems include a 785 nm laser.

https://doi.org/10.1021/acsomega.4c00591
ACS Omega 2024, 9, 50049−50063

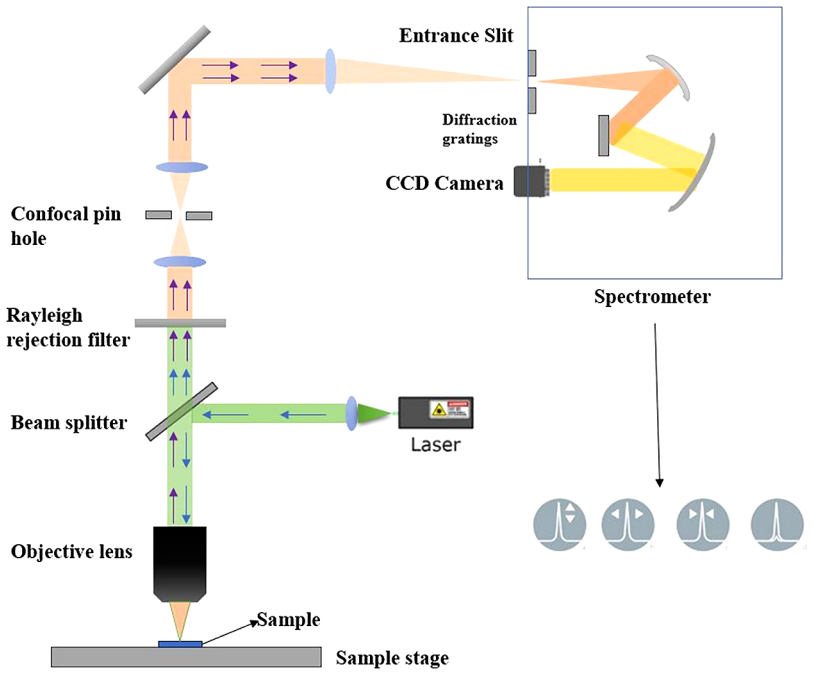

Figure 4. Schematic of experimental set up for confocal Raman spectroscopy.

Fiber optic cables are used to transport and collect laser energy from the sample. A notch or edge filter eliminates Rayleigh and anti-Stokes scattering, and the remaining Stokes scattered light is sent on to a dispersion element, generally holographic grating. A CCD detector catches the light, producing the Raman spectrum. Here we will explain all the details of components and their physical uses to obtain Raman spectra. The rest of the spectrometer receives the remaining Raman scattered light. Figure 4 shows the schematic of the experimental set up for Raman spectroscopy.

2.2.1. Excitation Source (Laser). We can use a number of lasers for example, helium−neon (He−Ne) (632.8 nm), argon ion (488 and 514.5 nm), Nd:YAG laser and Nd:YVO4 (1064 nm), near infrared (IR) diode lasers (785 and 830 nm), etc. Gas lasers, such as He−Ne lasers, operate at lower output power levels and longer wavelengths but are significantly cheaper to acquire and run. They also have good qualities in terms of beam quality, line width, and laser noise. Laser diodes come in a variety of emission wavelengths and are extremely small and dependable sources. Although high beam quality and narrow line width are easier to accomplish at low power levels, optimized diode lasers can have very high output power while maintaining high beam quality and small line width. One main drawback of diode laser is that their center wavelength may not always be the same frequency and sometimes may not be single-frequency. Continuous-wave diode-pumped lasers (DPL) have a set wavelength ranging from 457 to 1064 nm. Single frequency operation offers ultranarrow spectral line width, extended coherence length, and high spectral purity. The lasers are designed and built to be highly reliable. Quantum cascade lasers can be utilized to produce tunable mid-infrared light. Ar and Ar−Kr lasers are no longer commercially available. Various laser parameters, particularly the center wavelength and output power, should stay relatively steady during operation; otherwise, the precision and repeatability of spectroscopic observations may suffer. This is especially important when working with weak Raman scatterers, which necessitate extended measurement durations. Long wavelength sources, on the other hand, such as diode or Nd:YAG lasers, may operate at extremely high power without dissolving the material and can also erase or minimize fluorescence. A 532 nm green laser is the most often used laser in Raman spectroscopy because it has high sensitivity at a reasonable cost. The shorter the wavelength of the laser, the better the sensitivity. As a result, for investigations that need extreme sensitivity, a costlier 488 nm blue laser should be utilized instead. However, sensitivity is not the only element to consider while choosing a laser. Shorter wavelength lasers are more likely to cause the material to glow, interfering with the Raman spectra. If a material fluoresces when a 532 nm laser is employed, a 785 nm infrared laser will frequently perform better. The most often used laser wavelength in Raman spectroscopy is 785 nm, which provides modest fluorescence while maintaining a reasonably high Raman intensity. However, for items with strong fluorescence backgrounds, such as dyes, a 1064 nm laser may be required. Because of the reduced Raman intensity and potential of sample damage caused by a more powerful laser, this laser is typically employed only when the fluorescence is exceptionally high. Because most materials will not glow when exposed to the 785 nm laser, it is a fairly adaptable laser for most studies at the expense of some sensitivity. Longer wavelength lasers generate greater heat, which may harm the sample. This may be alleviated by lowering the laser's power, which regrettably reduces Raman sensitivity even further. That is why a 633 nm laser is an excellent choice for some investigations; the wavelength is sufficiently long to eliminate fluorescence but shorter than a 785 nm laser, so it does not overheat the material.

2.2.2. Optical Components. The light from the illuminated spot is focused by a microscopic objective (MO) and collimated by a lens before being routed to a notch filter and spectrometer to get the Raman spectrum. Raman laser line filters are intended to transmit a certain laser wavelength while

https://doi.org/10.1021/acsomega.4c00591
ACS Omega 2024, 9, 50049−50063

excluding all other ambient light. This bandpass filter effectively cleans the laser beam signal and eliminates noise. To get a good signal-to-noise ratio in Raman measurements, Rayleigh scattering must be blocked from reaching the detector while sending the Raman signal. To reject the background signal, you can use a double or triple grating spectrometer. Angle tuning narrow bandpass filters are useful for Raman imaging applications that demand a high signal throughput for a given Raman mode. The notion is based on the fact that the center wavelength of a narrow bandpass filter blueshifts as the angle of incidence increases. A single bandpass filter can cover more than 10% of the center wavelength at normal incidence. To optimize the Raman measurement, optical filters can be selected and customized based on the experiment's requirements. Long pass edge filters are used in Raman spectroscopy to transmit light from a Raman-scattered material at lower energy or longer wavelengths while blocking undesired Rayleigh scattered signal laser light. To do this, only wavelengths greater than a certain blocking wavelength are communicated. Most commercial Raman microscopes nowadays are equipped with long path filters.

2.2.3. Wavelength Selection (Filter). To isolate a single laser beam, bandpass filters are used. To get high-quality Raman spectra, it is usually necessary to use a laser rejection filter for distinguishing Raman scattered light from Rayleigh and reflected laser signals. Typically, notch filters are utilized for this purpose. Volume holographic filters,[27] on the other hand, are becoming increasingly widespread, allowing changes as small as 5 cm^{-1} to be noticed.

2.2.4. Detector. A visible spectrometer with software employs ultrahigh performance, high-sensitivity, and high resolution. 640 × 480 pixels, 1280 × 1024 pixels, 2048 × 64 pixels, the widely used camera resolution of 1600 × 1200 pixels frequently employs a slightly bigger sensor with 1/1.8″ and the same pixel size, a back-thinned CCD array, thermoelectrically cooled down to −5 °C. Sensor noise is reduced, and SNR is almost 2 times higher than others. Increased reliability ensures that the measurement results do not change with temperature.

Higher-sensitivity charge transfer devices (CTDs) like charge-coupled devices (CCDs) and charge-injection devices (CIDs) have been developed as a result of technical and instrument developments. There are many varieties of CCDs that are optimized for various wavelength ranges. Enhanced CCDs can be employed for weak signals along with pulsed lasers. The focal length of the spectrograph and the size of the CCD define the spectral range. CCDs require some cooling to be acceptable for high-quality spectroscopy. This is commonly accomplished using either Peltier cooling (usable for temperatures as low as −90 °C) or liquid nitrogen cryogenic cooling. Most Raman systems employ Peltier-cooled detectors; however, liquid nitrogen-cooled detectors provide benefits in some specialized applications. The Peltier effect is the inverse of the Seebeck effect; electrical current running through a junction connecting two materials emits or absorbs heat per unit time at the junction to balance the difference in chemical potential between the two materials. This phenomenon allows for the creation of an electrical refrigerator known as a Peltier cooler. Because of its lower cooling power than compressor-based freezers, the Peltier cooler has been used in specialized applications such as infrared detectors, CCDs, CPU coolers, wine cellars, and so on.[27,28]

Before reaching the CCD detector, the diffraction grating within the Raman spectrometer scatters the distinct wavelengths of Raman scattered light out in space. The number of lines on the diffraction grating may be changed to control how much or how little light is spread out. Diffraction gratings having a greater line density, or more lines per millimeter on the grating, will spread out the light more. Controlling how light passes through the detector is extremely useful for studying various parts of the Raman spectrum. Examining the entire Raman spectrum (100−3500 cm^{-1}) demands the use of a wide range of wavelengths. This is why a grating with a lower line density is necessary because lower line density diffraction gratings do not spread the light out as much, enabling a wider range of light to reach the detector. When the laser is altered for a Raman experiment, the diffraction grating may also need to be adjusted. Though the Raman shifts for a sample are constant, the wavelength of the laser influences the wavelength of Raman scattered light that reaches the detector. Examining a tiny portion of the spectrum necessitates the employment of a diffraction grating with a greater line density, causing the light to spread out more. This implies that less light will reach the detector overall, but we will be able to investigate certain areas of the spectrum in more detail, for example, with higher spectral resolution.

3. APPLICATIONS OF RAMAN SPECTROSCOPY IN BIOLOGY

3.1. Biomolecular Structure Determination: Unveiling Protein and Nucleic Acid Conformation. While imaging biological materials, Raman microscopy may thoroughly detect molecular species, such as lipids, proteins, and nucleic acids, and their spatial distributions in a sample.[29] The cytoplasm of living HeLa cells has been treated with a 532 nm laser, producing a Raman spectrum.[30−32] The strong peaks in the spectrum represent Raman scattering from the many vibrational modes of the molecules in the cells. Plotting the spatial distribution of peak intensities, which provides information on the molecular species present at the measurement spots, enables the creation of Raman images of the cells.[33] The visualization of lipid storage, lipid phase separation, axonal myelin, and tissue structures like the liver, brain, and skin have all been accomplished with success. High wavenumber areas (2800−3000 cm^{-1}) in particular offer stronger signals due to the vibrational modes of CH_2 and CH_3 in the cell.[34−38] The Raman spectra, which describe the molecular makeup at the measured locations, can be used to discriminate between organelles and cells in tissues and other components of a sample.[39] Multivariate analytical techniques can be utilized in addition to Raman peak mapping to separate nuclei, lipid droplets, and cell bodies and offer morphological information on the sample without labeling.[40−45] Multiple curve resolution and independent component analysis are two examples of these techniques.

3.2. Biophysics: Studying Protein Folding, Interactions, and Dynamics. Many biological processes are controlled by the large, complex molecules known as proteins. However, a number of deadly diseases can be brought on by protein dynamics. Understanding the structure and form of proteins is crucial. A mechanistic knowledge of the way proteins fold remains elusive despite various attempts. As a result, new methods are always being researched. Raman spectroscopy can be used to pinpoint particular amino acid residues like tyrosine, tryptophan, and phenylalanine as well as secondary protein structures including helices, beta-sheets, twists, and random structures in proteins.[33] Raman spectra can

https://doi.org/10.1021/acsomega.4c00591
ACS Omega 2024, 9, 50049−50063

be used to discriminate between lysozyme protein and bovine serum albumin (BSA) based on the differences in their primary, secondary, and tertiary sequences and structures. Although it is challenging to detect the structure of a protein using a Raman spectrum alone, spectra can be used to distinguish tiny changes in the conformations of proteins like BSA during melting. Numerous novel approaches to methodology and data analysis have been investigated in protein Raman spectroscopy investigations.

3.3. Cellular Analysis: Probing Molecular Composition and Dynamics. Raman spectra can be used to separate different types of cells as the spectral forms indicate the balance of chemical species at each location in a sample. The identification of cancerous cells and tissues is one of the practical uses of this technique, which has been demonstrated to be effective for a variety of tumor forms.[46] The label-free approach is the subject of in-depth study for intraoperational rapid diagnostics.[47,48] Raman microscopy is expected to demonstrate dynamic changes in intracellular chemical compositions during cell differentiation or reprogramming in the same way that induced pluripotent stem (iPS) cells, osteoblasts, and embryonic stem (ES) cells.[49−53] In these studies, the gradual changes in chemical composition throughout the modulation of cellular states were visualized by the multivariate analysis of Raman spectra obtained at multiple time points as the cell state changed. Due to its capacity to identify cellular states without the use of labels, Raman microscopy is predicted to be a successful technology for the assessment and quality control of cells for use in regenerative medicine and drug development. It has been demonstrated that comparable techniques may distinguish between various immune-stimulated cell responses. Raman spectra may distinguish between various cell states; however, the biological background that is detected in Raman experiments is difficult to pinpoint. This paves the way for the omics-equivalent analysis of live cells and tissues as well as the employment of Raman microscopy as a reliable tool for comprehending living systems.[54−56] The relationship between Raman spectra and gene expression in cells has recently been investigated using a combination of transcriptome and Raman microscopy. The integration with flow cytometry is one of the predicted Raman microscopy applications for biological and medicinal applications.[57−59] This technique enables live cell applications by allowing cells to be sorted according to their characteristics and functions without the need for labels.[60−62]

3.4. Disease Diagnosis: Detection of Biomarkers and Pathological Changes. To detect stomach cancer, doctors currently use endoscopic diagnostics, histology, clinical imaging, tumor markers, and other clinical methods. Endoscopic and histological testing, which is carried out on a tissue and cellular level, is the "gold standard" in clinical tumor diagnosis. After staining the tissues, it is possible to distinguish between healthy gastric mucosa, precancerous lesions, and stomach cancer based on the kind, quantity, and arrangement of the glands as well as the nucleoplasmic ratio of the cells. However, in order to do so, a biopsy sample is required, which may result in intestinal bleeding or perforation. Additionally, testing processes take time, and the subjective factors of the pathologists might affect how precisely a pathological diagnosis is established, delaying the results. Despite being frequently used as clinical diagnostic tools, X-ray contrast radiography examination, computed tomography examination, magnetic resonance imaging (MRI), and other imaging diagnostic procedures are limited in their capacity to assess the structure and makeup of problematic tissues. These methods have a low detection rate for microscopic tumors and early gastric cancer due to their inadequate capacity to discern the shape and structure of sick tissues and their limited spatial resolution. Commonly used clinical indicators include CEA, CA19-9, CA125, CA72-4, etc. Due to their low specificity and sensitivity, tumor markers have limited usefulness in the early identification of gastric cancer since they are subject to individual variations and some benign diseases. The detection process requires some time. But locating tumor markers is quite difficult. This demonstrates the value of Raman spectroscopy in the early detection of stomach cancer. The composition and concentration of chemical substances in stomach tissues or cells, which will vary to some amount during the malignant process, can be directly related to the matching distinctive peaks and intensities of the Raman spectra. The total sensitivity and specificity of Raman spectroscopy for the diagnosis of stomach cancer are 0.89 and 0.92, respectively, when histology is used as the reference standard. Raman spectroscopy thus offers a noninvasive, precise, and user-friendly optical diagnostic tool for the sensitive and objective early identification of stomach cancer.[63] Nowadays, surgically excised tissues, isolated cell samples, body fluids, or endoscopic biopsies make up the majority of the samples used in stomach cancer Raman research. Spontaneous Raman spectroscopy using lasers with a wavelength of 532 nm, 785 nm, or 1064 nm is the main technique for collecting spectrum data for the in vitro study of tissue or cell samples.[64,65] Additionally, confocal Raman spectroscopy techniques have been used in a number of studies. These techniques have the advantage of great spatial resolution and effectively remove signal interference from layers outside the focal plane. Surface-enhanced Raman spectroscopy (SERS), with a maximum amplification of 10^{15} times over ordinary Raman spectra of molecules, was mainly used to investigate substances like blood,[66] breath, and saliva.[67] Additionally, fiber optic Raman spectroscopy, which makes use of in vivo fiber optic probes, is essential for the in situ analysis and real-time detection of gastric cancer patients.

In recent modern societies chronic kidney disease constitutes one of the most frequent noncommunicable disease pathologies. As reported by the World Health Organisation, 10% of the world's population suffers from chronic kidney disease, with millions dying each year as a result of kidney failure. Kidney failure causes water, electrolyte, and nitrogen breakdown, as well as other metabolic abnormalities in the human body. One of the key developments in therapeutic fields is the investigation of changes in the composition of distinct human skin layers. Furthermore, the skin is easily accessible and hence appealing as an in vivo diagnostic object. Bratchenko et al. reported the most significant detection of kidney failure by Raman spectroscopy of in vivo human skin analysis.[68] This in vivo investigation of skin spectral characteristics in kidney failure patients uses conventional Raman spectroscopy in the near-infrared range. In terms of identifying the target subjects with kidney failure, the use of Raman spectroscopy on the forearm skin of adult patients with kidney failure (90 spectra) and healthy adult volunteers (80 spectra) yielded. The experimental data set was submitted to discriminant analysis using latent structure projection (PLS-DA). When applying the PLS-DA approach to identify participants with kidney disease, the most relevant Raman

https://doi.org/10.1021/acsomega.4c00591
ACS Omega 2024, 9, 50049−50063

spectral bands are 1315−1330 cm^{-1}, 1450−1460 cm^{-1}, and 1700−1800 cm^{-1}. These bands correspond to amide I, amide III and the δ(CH2) bending vibrations in α-helix collagen.

3.5. Raman Imaging and Mapping: Visualizing Biological Samples at the Molecular Level. In vitro gastric tissue and cell using Raman spectroscopy: The data gathering and classification of stomach tissues or cells is the most direct and frequent application of Raman spectroscopy in figuring out the type of gastric cancers. In contrast to the standard intraoperative histological diagnosis, which requires procedures including tissue transport, sample processing, section preparation, and tissue identification, the Raman spectroscopy-based gastric cancer diagnostic technique is able to collect data directly from fresh tissues. The most frequent types of samples employed in Raman analyses of isolated stomach tissues and cells include frozen samples, formalin-fixed paraffin-embedded (FFPE) samples, and fresh tissue samples.[69] FFPE samples can be analyzed once the findings of the diagnostic tests are known, albeit the fixation of the tissue may modify its biochemical composition and lead to changes in Raman peaks.[65,70−75] The signal-to-noise ratio and reproducibility of the Raman spectra of frozen tissues are excellent, and they resemble those of fresh tissues more.[76,77] The intensity of multiple Raman peaks, however, seems to change during the freezing and thawing process, making identification less accurate than in fresh tissues.[78,79] Raman spectroscopy of isolated tissues is routinely performed using desktop Raman spectroscopy equipment. Due to the relatively low absorption coefficient of NIR light by molecules in biological tissues that typically absorb light (e.g., melanin, water, and lipids), NIR light sources, particularly 785 nm lasers positioned in the high transmittance "optical window" of biological tissues, are frequently used in medical Raman measurement systems.[69] While NIR light with wavelengths of 785 nm and 1064 nm is useful in lowering tissue autofluorescence and has been employed more frequently in diagnostic tests for stomach cancer, visible light with a wavelength of 532 nm has a higher scattering intensity.[70−72] The sample is illuminated by the transmission system, and the Raman signal produced by the illuminated tissue sample is then collected and analyzed by the detector and spectrometer. The Raman fingerprint region (FP, 400−1800 cm^{-1}), the high wavenumber region (HW, 2800−3200 cm^{-1}), and the intermediate region which is often devoid of Raman distinctive peaks can be distinguished within this wavenumber range. Raman spectra are commonly recorded between 400 and 3500 cm^{-1}. The majority of studies only collect spectrum data in the FP area or in both the FP and HW regions since the acquisition range of the spectra influences the acquisition time and redundancy of future data processing. In a related investigation, it was discovered that FP and HW region analysis was superior to HW region analysis alone and preferred to FP and HW region analysis separately.[71,80] Additionally, studies have shown that while lengthening the integration period can significantly improve prediction accuracy, doing so at the expense of laser intensity has no effect on overall prediction accuracy.[81] The diagnostic results may be affected by the use of different spectrum ranges and spectral acquisition parameters; as a result, the ideal experimental circumstances should be established by the characteristics of the sample being used in the experiment. As a rapid and noninvasive method for detecting stomach tissues, Raman spectroscopy has made tremendous progress. Other studies have shown that with utilizing Raman detection of isolated stomach tissues, it is possible to identify malignant gastric mucosal tissues, diagnose gastric dysplasia, differentiate the stage of gastric adenocarcinoma, and discriminate between precancerous and cancerous tissues.[74] Additionally, researchers investigated how the genomic DNA, nuclei, and tissues of normal and malignant gastric mucosa affected the spatial organization and biochemical composition of mucosal tissue during carcinogenesis by looking at variations in the typical peak spectra of these components.[82] Researchers demonstrated that NIR Raman spectroscopy can be used to detect *Helicobacter pylori* infection and inflammatory damage in the stomach at the molecular level. On the scale of detection, cells are more refined than tissues.[83] Researchers identified probable stomach mucosal cancer cells using Raman spectroscopy on cultured single cells.[64] Nondestructive Raman spectroscopy was used to monitor apoptosis in gastric cancer cells and test new medications against the therapeutic effects of various cancer cells after discovering the primary compositional differences between apoptosis-inducing cells and gastric cancer cells.[84]

3.6. Microbiology: Identification and Differentiation of Microorganisms. Raman spectroscopy has been intensively studied in terms of its potential applications in clinical studies because the sample preparation procedures are simple and the spectroscopic operations may be completed in only a few seconds, so it is a promising tool for diagnosing bacterial disease.[85] Raman spectroscopy cannot completely replace conventional laboratory procedures since there is still a considerable gap between basic research and practical application. Examples include the weak Raman effect, which calls for prolonged measurement times, and sample fluorescence, which brings noisy signals into the spectrum and makes subsequent analysis more difficult.[86] Additionally, heated samples can be destroyed and have their Raman spectra changed by intense laser radiation. It is advised to study biological samples in aqueous solutions or with low-energy near-infrared light, such as that with wavelengths of 785 or 830 nm.[87] During the analysis of bacterial samples, Raman spectroscopy provides information on both chemical compositions and biomolecular structures, such as DNA, RNA, proteins, lipids, and carbohydrates. The term "whole-organism fingerprint" is frequently used to describe this information. For instance, the amide I vibration at 1665 cm^{-1} is the main signal for proteins, but the Raman signals for C−H stretching at 2930 cm^{-1} and C−H deformation at 1440 cm^{-1} are both present.[88,89] Additionally, single-bacteria analysis and live-bacteria research have both utilized Raman spectroscopy to lessen the metabolic variability of bacteria at various phases and to better comprehend cellular dynamics.[90,91] It was established that particular peaks at 540 and 1380 cm^{-1} differed significantly between Gram-positive and Gram-negative bacteria. The glycosidic linkages in N-acetyl glucosamine and N-acetyl muramic acid of peptidoglycan were principally responsible for these variations.[92] Research employing Raman spectroscopy on clinical bacterial infections has thus far required growth on agar plates because of the low bacterial content in clinical samples.

3.7. Biomedical Engineering: Applications in Tissue Engineering and Regenerative Medicine. *3.7.1. Applications of Raman Spectroscopy to Tissue Engineering.* Tissue engineering (TE) holds great promise for improving the prognosis of patients with degenerative illnesses. Successful clinical translation of TE as a therapy component requires

https://doi.org/10.1021/acsomega.4c00591
ACS Omega 2024, 9, 50049−50063

describing and quantifying tissue creation and contrasting the TE implant with native tissue. For instance, conventional approaches rely on histological labeling and biochemical assays, both of which have inherent risks, to determine the extracellular matrix (ECM) composition in orthopedic TE, such as cartilage or meniscus. These methods are not suitable for in-depth analyses of ECM component distributions since they include labeling, are still qualitative or semiquantitative, and are still qualitative in nature. To use these methods to measure tissue growth over time, a translational system would also require the concurrent generation of sacrificial designed tissue samples. Thus, there is an urgent unmet demand to include cutting-edge optical techniques like Raman spectroscopy into TE. Raman spectroscopy may be essential in TE for biomolecular characterization, comparisons with natural tissues, and quality control of live cell TE production.[93] Raman spectroscopy has not been extensively studied for bimolecular TE structure evaluation. Additionally, they have investigated the synthesis of ECM in polymeric scaffolds and samples cultured in chondrocyte medium using Raman spectroscopy and complementary techniques.[93] Raman spectroscopy was used to spot spectrum changes in thermally stressed tissue 3 weeks after implantation in mice.[94] With the use of Raman microspectroscopy, the mineralized nodules created in vitro was studied.[95] In contrast to osteoblasts and adult stem cells, which exhibited biological characteristics specific to bone, the bone nodules produced by embryonic stem cells lacked the complex biomolecular and mineral composition evident in the original tissue. In order to evaluate the ECM microstructure and biomolecules (such as collagen, glycosaminoglycans (GAGs), and hydration) of sectioned native articular cartilage and TE constructions, researchers devised a polarized Raman imaging technique.[96] On the basis of collagen alignment and the molecular signature, this research demonstrated that actual bovine tissues were connected to greater zonal complexity (at least six separate zones could be differentiated). In both natural and tissue-engineered structures, the pure spectra of water, GAGs, and collagen were separated using multivariate curve resolution (MCR). In light of depth-dependent biomolecular structure, they were able to develop quantitative criteria for contrasting native and TE constructs.

3.7.2. Raman Spectroscopy Applications in Regenerative Medicine. Raman spectroscopy has a wide range of potential applications in regenerative medicine due to its adaptability; some of the most important ones are listed here.

3.7.2.1. Applications of Raman Spectroscopy to Stem Cells. Just two of the many limitations on the use of stem cells in research and the therapeutic setting are the unpredictability of cell populations and the lack of clarity regarding stem cell quality.[97] For this area of study and therapy, noninvasive techniques for defining cell types, identifying disease or apoptotic states, and evaluating differentiation would be necessary. All these elements make Raman spectroscopy promising, and it has proven that it is suitable for studying a range of regeneration-related topics. This is made possible by its ability to evaluate biomolecular composition. Teratomas, which are tumors made up of many cell types, may form after therapy if differentiated cells are coexisting with undifferentiated stem cells.[98,99] It has been possible to discriminate between stem cells and their offspring using Raman spectroscopy. Currently, a number of methods are used to find stem cells, including harmful immunocytochemical methods that make use of fluorescence.[100] To discriminate between human embryonic stem cells (hESCs) and their cardiomyocyte progeny, scientists performed multivariate data analysis of their Raman spectra.[101] Spectrum of human embryonic stem cells (hESCs) resembles that of human-induced pluripotent stem cells more so than it does that of their differentiated progeny.[102] In order to identify both from adipose-derived stem cells, CARS microscopy used to see the lipids in adipocytes and the mineralization in osteoblasts.[98]

3.7.2.2. Applications of Raman Spectroscopy to Cell Lines. The challenges of producing stem cells are typically overcome in regenerative medicine research via the use of cell lines. Determining the quality of the cells and establishing that the phenotypes of cell lines genuinely match the cells they are intended to copy have proven to be challenging tasks. When scientists compared cell lines to primary stem cells using single-cell Raman spectroscopy, they discovered that the metabolic profiles of A549 adenocarcinoma cells and the alveolar type II (ATII) epithelial cells they are intended to mimic are extremely different.[103] In the meanwhile, the alveolar type I-like cell line TT1 offers a respectable depiction of ATI. This highlights how general biochemical changes between cells may be swiftly and noninvasively studied using Raman spectroscopy. Spontaneous Raman spectroscopy was employed to distinguish between live and dead cells in an effort to noninvasively test cell viability.[104−106] Changes in the DNA-attributed peaks at 782, 788, and 1095 cm^{-1} could be used to determine the stage of the cell cycle of a particular cell. Dead cells had unusually low DNA peak intensities and changed protein peak intensities, possibly as a result of modified protein structure.

3.8. Surface Enhanced Raman Spectroscopy (SERS) in Biological Applications. Surface-enhanced Raman spectroscopy (SERS) is a very sensitive method for increasing the Raman scattering of molecules supported by nanostructured materials. SERS enables the structural fingerprinting of low-concentration analytes via plasmon-mediated amplification of electrical fields or chemical augmentation. Because of its extremely high sensitivity and selectivity, SERS has a wide range of applications in surface and interface chemistry, nanotechnology, biology, biomedicine, food science, and other fields.[107−111] The Raman spectra of pyridine on roughened silver were originally seen in 1974;[112] however, at the time, the authors did not recognize that these spectra were caused by any uncommon, increased, or novel processes. Since its development in 1977,[113] interest in and use of surface-enhanced Raman spectroscopy (SERS) has increased tremendously. In particular, the advancement of nanotechnology has accelerated the advancement of SERS technology. It has grown in popularity in the scientific community, and it has inspired several different spectroscopic techniques that use heightened local fields caused by plasmon excitation in the NPs to study optical phenomena such as fluorescence or nonlinear optics. Furthermore, connecting SERS with AFM or STM tips has resulted in tip-enhanced Raman scattering (TERS), a strong imaging technique.[114] For analytical applications, SERS stands out from many other techniques because of the extensive vibrational spectroscopic information it gives, which has led to applications in various domains such as electrochemistry, catalysis, biology, medicine, and others. In a further sensing technique, SERS tags made of plasmonic nanoparticles (NPs), Raman reporter molecules, and recognition components are used as stable and brilliant labels in, e.g., DNA detection

https://doi.org/10.1021/acsomega.4c00591
ACS Omega 2024, 9, 50049−50063

schemes or immunoassays.[115−117] SERS has shown significant promise in protein identification and quantification. However, the low spectrum repeatability resulting from random protein immobilization on SERS substrates makes it difficult for SERS to explore protein activities in the absence of exogenous Raman labels. SERS can be applicable to investigate the conformational fluctuation of single proteins,[118] which is one of the very first detailed SERS study on proteins. Also, live cell surface-enhanced endoscopic probes made of plasmonic nanowire waveguides are used to perform SERS. It has been established that probe insertion does not stress the cell. Unlike traditional SERS endoscopy, which excites at the cell's hotspot, the distant excitation approach produces low-background SERS spectra from particular cell compartments with minimum photodamage.[118] This is the first report of SERS detection inside a single cell using an endoscopy approach, which breaks the limitation of SERS in cells. In recent times knowing the dynamics and distribution of medicinal medicines in live cells is critical for designing and developing therapies. However, the methods available to uncover this information are relatively restricted. SERS endoscopy, using plasmonic nanowires as SERS probes, was used to monitor the intracellular fate and dynamics of doxorubicin, a common chemo-drug, in A549 cancer cells.[119] Figure 5 shows the SERS-based potential biological applications.

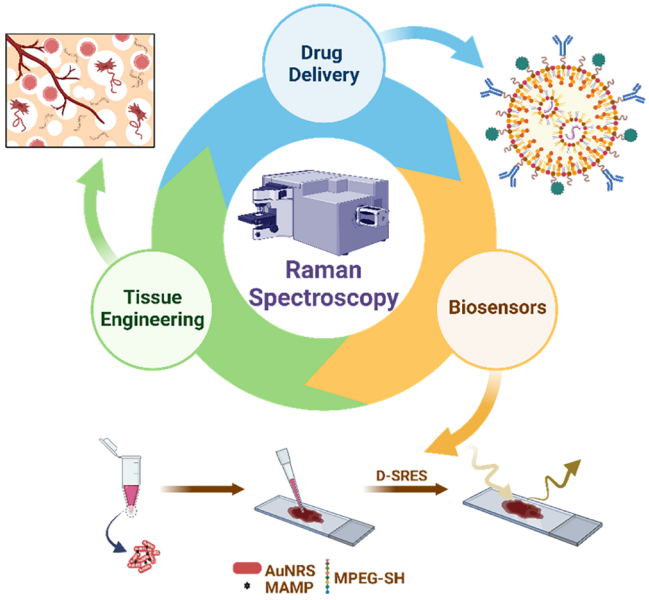

Figure 5. Surface-enhanced Raman spectroscopy (SERS) based biological applications. (Created with BioRender.com.)

Figure S1 shows the different Raman spectroscopic techniques applied in the development of biology.

4. CHALLENGES IN RAMAN SPECTROSCOPY FOR BIOLOGICAL RESEARCH

4.1.1. Sample Preparation and Handling. For applications based on Raman microscopy, sample processing compatibility must always be taken into account. Raman spectroscopy's great compatibility with aquatic environments is one of its main advantages. In buffered saline solution, imaging can therefore be carried out directly on hydrated tissues without the need for sample processing (such as fixation, dehydration, or embedding).[96] It is typically desirable to explore specimens with flat surfaces for the capture of large hyperspectral photographs in order to keep a stable focus over a broad region of interest. Using a vibratome or cutting block, or a cryostat if tissue viability preservation is required, sample flattening is easily performed. Traditional histology sectioning techniques can also be used to cut tissues into sections.[120] Paraffin embedding is unsuitable for Raman acquisitions to considerable spectrum interference, which is one disadvantage of Raman imaging. Strategies for experimental and digital deparaffinization have both been investigated.[121,122] Despite the fact that molecular cross-linking brought on by formalin fixation leads in very modest changes in the Raman spectra, tissues can be easily scanned in both a fresh and fixed state. The use of specialized substrates, such as aluminum, steel, calcium fluoride (CaF_2), or magnesium fluoride (MgF_2, which induces a negligible background signal), is typically required for nonconfocal Raman spectroscopy, which cannot be performed on conventional microscopy glass slides.[123,124] Modern confocal Raman microscopy with high magnification objectives and a narrow aperture, however, provides imaging with basically minimal contribution from common glass substrate, even for imaging a monolayer of cells.[125]

4.1.2. Data Acquisition and Analysis. To extract molecular information from the enormous amount of data obtained from hyperspectral Raman pictures, computational processing is required. Before analysis, Raman spectra must be preprocessed to get rid of distracting components such background autofluorescence and noise. Techniques used for this include cosmic ray rejection, autofluorescence subtraction, dark signal subtraction, and normalization.[126−128] Additionally, system response adjustment using NIST standards, such as the standard reference materials range (for example, SRM2241 for 785 nm laser excitation), should typically be used to standardize the Raman intensities. This will improve consistency between instruments. Semiquantitative images can be created from the absolute signal for sufficiently flat samples, but for samples with thickness changes, spectral normalization techniques may be needed to provide artifact-free images. Raman images taken at several periods must occasionally be combined in temporal research in order to perform quantitative image analysis. This necessitates stringent standardization of the Raman pictures, such as through spectrum normalization, due to the varying focus of the microscope objective and, consequently, the different absolute intensities.[125,128] Historically, Pearson's correlation coefficients (PCCs) were utilized to locate Raman peaks.[129] The development of computational analytic techniques has come a long way. However, in recent years, machine learning and deep learning approaches have gained popularity.[130] Nowadays machine learning based analysis of single cell based Raman fingerprinting is being done.[131] There are several approaches to performing spectrum analysis on Raman images in general. Univariate peak analysis, which maps the intensities of a single Raman peak and also includes Gaussian peak fitting and peak intensity ratios, is the most basic technique. To extract precise quantitative data for particular ECM elements, more advanced multivariate or machine learning algorithms might be applied.[96] Since multivariate and machine learning consider the entire spectrum of spectral information, they generally offer more accurate quantitative analysis. Supervised analysis and unsupervised analysis are the two primary versions of these approaches.

https://doi.org/10.1021/acsomega.4c00591
ACS Omega 2024, 9, 50049−50063

4.1.3. Limitations and Potential Artifacts. One of the main issues with Raman spectroscopy is the inability to identify signals. A material's low Raman activity, weak Raman signal emission, or fluorescence-overpowering signal can all contribute to low detection. The first of them cannot be addressed without changing the sample, but the other two can be (using SERS, for example). Once a signal is found, Raman has few limitations. (A) Raman spectrometers are unable to distinguish between chemicals with high color and those that are noncovalently bound. The majority of samples in critical Raman application fields (such pharmaceutical quality control and hazardous substance identification) are Raman active, despite the fact that HCl and NaCl are notable outliers. (B) The observation of a Raman event occurring once every 10^6 excitation photons on average places restrictions on the method's sensitivity and usefulness for contamination identification or trace analysis. One method that can occasionally be used to amplify weak signals is surface-enhanced Raman spectroscopy (SERS). The use of beam enhancer technology in conjunction with transmission Raman spectroscopy (TRS) is a possibility. (C) Fluorescence, a far more efficient optical technique, can be used to mask Raman bands in the spectrum. Options for mitigation, including the use of longer wavelength excitation sources, are frequently accessible for the examination of materials with high fluorescence. SORS is particularly helpful for minimizing fluorescence while taking measurements through containers.

5. EMERGING TRENDS AND FUTURE DIRECTIONS IN RAMAN SPECTROSCOPY FOR BIOLOGICAL RESEARCH

Because the current disease detection techniques have substantial shortcomings, there is an urgent need to develop new technologies that can diagnose diseases swiftly. Label-free illness diagnosis is made possible by a cutting-edge method known as Raman spectroscopy, which can identify differences in chemical composition across various types of materials. Raman spectroscopy is used to distinguish at the molecular level between healthy and unhealthy materials, enabling the early detection of cancer. Analyzing the chemical makeup and structural alterations of isolated tissue or physiological fluid samples allows for this. Real-time in vivo detection is made possible by the integration of a Raman fiber optic probe and endoscope, helping to determine the location and amount of cancer development. The effectiveness and precision of Raman spectroscopy in the detection of stomach cancer are also steadily improving thanks to advancements in Raman spectrometer technology and novel techniques developed from Raman data analysis. Although there have been substantial improvements in the diagnosis of stomach cancer, Raman spectroscopy still has several problems. Among the challenges are the development of a database and evaluation system for Raman spectra relevant to cancer, the elimination of spectral irregularities brought on by various spectrometers, and the acquisition of higher quality Raman spectra. In order to capture Raman spectrum data more quickly, it is still a challenge that needs to be investigated how to obtain higher-quality Raman spectra. The spectra obtained by various Raman spectrometers differ due to signal noise and laser stability. During Raman signal collection, the acquisition parameters, such as the laser's wavelength, power, and integration time, as well as various sample processing techniques, will affect the signal. In order to achieve detection repeatability and stability, adopting a standardized sample strategy and looking into data collection techniques are some of the main research objectives. To determine the variability of Raman peaks, the currently used data processing techniques are comparatively insufficient. Large or enormous volumes of spectral data require the development of more precise and dependable data processing algorithms. Processing Raman spectrum and Raman imaging data using computer science and technology, such as deep learning, provides several advantages. These technologies might eventually even replace pathologists in the detection of many cancer forms. Last but not least, despite the fact that Raman spectroscopy is very accurate at differentiating between healthy and malignant tissues, this accuracy is insufficient to detect the benignity and malignancy of tumors for the precise diagnosis of patient's tumors, necessitating a deeper investigation into how to use Raman spectroscopy for the diagnosis of cancer subtypes and stages. The development of innovative, rapid procedures for tumor diagnosis is a key step toward in situ real-time tumor diagnostics employing fiber optics and endoscopy. Numerous investigations have already used Raman endoscopy, but more in vitro testing is necessary before it can be applied in clinical settings. In conclusion, the Raman spectroscopy-based methodology has numerous potential uses in the detection of cancer, and is quickly becoming a recognized clinical diagnosis tool.

Table S1 shows the applications of Raman spectroscopy in biology and its advantages.

6. CONCLUSION

Undoubtedly, Raman spectroscopy has firmly established itself as an essential instrument inside the continuously progressing realm of biological investigation. It is employed as a noninvasive, label-free, chemically selective, imaging technique with recent advances enabling the probing of molecular orientation and chemical composition. This review has provided a comprehensive exploration of the fundamental concepts underlying Raman scattering, as well as an extensive examination of its wide-ranging applications, from gaining insight into the composition of cells, the structures of biomolecules, the diagnosis of diseases to the production of pharmaceuticals. The utilization of Raman imaging has significantly broadened our understanding of biological material by facilitating visualization at the molecular level. The inclusion of methodological aspects, such as sample preparation and data processing, serves as a reminder of the meticulousness and caution necessary when utilizing Raman spectroscopy in biological research. The advent of emerging trends, such as biosensing and point-of-care diagnostics, holds great potential for offering novel answers to enduring challenges. The integration of Raman spectroscopy into the fields of tissue engineering and regenerative medicine has the capacity to significantly transform the healthcare industry. Furthermore, within the field of neurology, Raman spectroscopy is positioned to elucidate the enigmatic intricacies of the brain's neural networks. This review has provided a complete overview of the transformational impact of Raman spectroscopy in the field of biological research. This phenomenon stands as evidence of the collaborative efforts by spectroscopists, biologists, and doctors from many disciplines. In the realm of expanding possibilities, Raman spectroscopy persists as an invaluable tool, shedding light on the trajectory toward enhanced comprehension and pioneering advancements within the field of biological sciences. The nascent stage of the

https://doi.org/10.1021/acsomega.4c00591
ACS Omega 2024, 9, 50049−50063

journey signifies the immense potential and prospects that lie ahead for Raman spectroscopy in the realm of biological study.

■ ASSOCIATED CONTENT

Supporting Information

The Supporting Information is available free of charge at https://pubs.acs.org/doi/10.1021/acsomega.4c00591.

(Figure S1) Raman spectroscopic techniques application in the field of biology and (Table S1) different applications of Raman spectroscopy in biology and its advantages (PDF)

■ AUTHOR INFORMATION

Corresponding Author

Shilpi Agarwal − *School of Physical Sciences, Jawaharlal Nehru University, New Delhi 110067, India;* orcid.org/0000-0002-1696-2605; Email: shilpiagarwal@mail.jnu.ac.in, sipi.agarwal@gmail.com

Authors

Anshuman Chandra − *School of Physical Sciences, Jawaharlal Nehru University, New Delhi 110067, India*

Vimal Kumar − *Department of Anatomy, All India Institute of Medical Sciences, New Delhi 110029, India*

Umesh Chandra Garnaik − *School of Physical Sciences, Jawaharlal Nehru University, New Delhi 110067, India*

Rima Dada − *Department of Anatomy, All India Institute of Medical Sciences, New Delhi 110029, India*

Imteyaz Qamar − *School of Biotechnology, Gautam Buddha University, Greater Noida, U.P. 201312, India*

Vijay Kumar Goel − *School of Physical Sciences, Jawaharlal Nehru University, New Delhi 110067, India*

Complete contact information is available at: https://pubs.acs.org/10.1021/acsomega.4c00591

Notes

The authors declare no competing financial interest.

■ ACKNOWLEDGMENTS

The authors acknowledge financial assistance from the DHR-ICMR (R.12014/30/2022) and DST (Project DST/TDT/DDP-47/2021), Government of India.

■ REFERENCES

(1) Hazle, M.A.; et al. Practical Raman Spectroscopy D.J. Gardiner and P.R. Graves (Eds.), Springer Verlag, Berlin, 1989 (ISBN 3-540-50254-8). viii + 157 pp. Price DM 78.00. *Vib. Spectrosc.* **1990**, *240*, 104.

(2) Smekal, A. Zur Quantentheorie der Dispersion. *Naturwissenschaften* **1923**, *11*, 873−875.

(3) Battimelli, G. Franco Rasetti. *Phys. Today* **2002**, *55* (12), 76−78.

(4) Brandmüller, J. Rayleigh-Streuung und Rotations-Raman-Effekt von Flüssigkeiten. *Zeitschrift Für Physik* **1955**, *140*, 75−91.

(5) De Gelder, J.; De Gussem, K.; Vandenabeele, P.; Moens, L. Reference database of Raman spectra of biological molecules. *J. Raman Spectrosc.* **2007**, *38*, 1133−1147.

(6) Carey, P. R. *Biochemical Applications of Raman and Resonance Raman Spectroscopes. Academic Press*, 1982, DOI: 10.1016/B978-0-12-159650-7.X5001-9.

(7) Sikirzhytskaya, A.; Sikirzhytski, V.; Pérez-Almodóvar, L.; Lednev, I. K. Raman spectroscopy for the identification of body fluid traces: Semen and vaginal fluid mixture. *Forensic Chemistry* **2023**, *32*, 100468.

(8) Muro, C. K.; Lednev, I. K. Race Differentiation Based on Raman Spectroscopy of Semen Traces for Forensic Purposes. *Anal. Chem.* **2017**, *89*, 4344−4348.

(9) Garnaik, U. C., Agarwal, S. Surface Enhanced Raman Spectroscopy for Alzheimer's Disease Diagnosis. In *Optica Sensing Congress 2023 (AIS, FTS, HISE, Sensors, ES)*; Technical Digest Series; Optica Publishing Group, 2023; paper STu5D.7, DOI: 10.1364/sensors.2023.stu5d.7.

(10) Garnaik, U. C.; Agarwal, S. Raman Spectroscopy as a Potential Tool to Analyze Alzheimer's Disease Progression. *Springer Proceedings in Materials* **2023**, *28*, 221−225.

(11) Devitt, G.; Howard, K.; Mudher, A.; Mahajan, S. Raman Spectroscopy: An Emerging Tool in Neurodegenerative Disease Research and Diagnosis. *ACS Chem. Neurosci.* **2018**, *9*, 404−420.

(12) Shipp, D. W.; Sinjab, F.; Notingher, I. Raman spectroscopy: techniques and applications in the life sciences. *Adv. Opt Photonics* **2017**, *9*, 315−428.

(13) Lee, J. H.; Kim, D. H.; Song, W. K.; Oh, M.-K.; Ko, D.-K. Label-free imaging and quantitative chemical analysis of Alzheimer's disease brain samples with multimodal multiphoton nonlinear optical microspectroscopy. *J. Biomed Opt* **2015**, *20*, 056013.

(14) Dong, J.; Atwood, C. S.; Anderson, V. E.; Siedlak, S. L.; Smith, M. A.; Perry, G.; et al. Metal binding and oxidation of amyloid-β within isolated senile plaque cores: Raman microscopic evidence. *Biochemistry* **2003**, *42*, 2768−73.

(15) Dhillon, N.; Garnaik, U. C.; Yadav, D.; Gupta, R.; Agarwal, S. Analysis of a therapeutic rich phytopharmaceutical compound of Azadirachta indica. *Spectrosc. Lett.* **2024**, *57* (11), 122−127.

(16) Gupta, S.; Huang, C. H.; Singh, G. P.; Park, B. S.; Chua, N. H.; Ram, R. J. Portable Raman leaf-clip sensor for rapid detection of plant stress. *Sci. Rep* **2020**, *10*, No. 20206.

(17) Chou, I. H.; Benford, M.; Beier, H. T.; Coté, G. L.; Wang, M.; Jing, N.; et al. Nanofluidic biosensing for β-amyloid detection using surface enhanced raman spectroscopy. *Nano Lett.* **2008**, *8*, 1729−35.

(18) Maiti, N. C.; Apetri, M. M.; Zagorski, M. G.; Carey, P. R.; Anderson, V. E. Raman Spectroscopic Characterization of Secondary Structure in Natively Unfolded Proteins: α-Synuclein. *J. Am. Chem. Soc.* **2004**, *126*, 2399−2408.

(19) Schipper, H. M.; Kwok, C. S.; Rosendahl, S. M.; Bandilla, D.; Maes, O.; Melmed, C.; et al. Spectroscopy of human plasma for diagnosis of idiopathic Parkinson's disease. *Biomark Med.* **2008**, *2*, 229−38.

(20) Utzinger, U.; Heintzelman, D. L.; Mahadevan-Jansen, A.; Malpica, A.; Follen, M.; Richards-Kortum, R. Near-infrared Raman spectroscopy for in vivo detection of cervical precancers. *Appl. Spectrosc.* **2001**, *55*, 955−959.

(21) Short, K. W.; Carpenter, S.; Freyer, J. P.; Mourant, J. R. Raman spectroscopy detects biochemical changes due to proliferation in mammalian cell cultures. *Biophys. J.* **2005**, *88* (6), 4274−88.

(22) Koljenović, S.; Schut, T. B.; Vincent, A.; Kros, J. M.; Puppels, G. J. Detection of meningioma in dura mater by Raman spectroscopy. *Anal. Chem.* **2005**, *77* (24), 7958−65.

(23) Jalkanen, K. J.; Wurtz Jurgensen, V.; Claussen, A.; Rahim, A.; Jensen, G. M.; Wade, R. C.; Nardi, F.; Jung, C.; Degtyarenko, I. M.; Nieminen, R. M.; Herrmann, F.; Knapp-Mohammady, M.; Niehaus, T. A.; Frimand, K.; Suhai, S.; et al. Use of vibrational spectroscopy to study protein and DNA structure, hydration, and binding of biomolecules: A combined theoretical and experimental approach. *Int. J. Quantum Chem.* **2006**, *106*, 1160−1198.

(24) Raman, C. V.; Krishnan, K. S. A new type of secondary radiation [11]. *Nature* **1928**, *121*, 501−502.

(25) Hanlan, J.; Skoog, D. A.; West, D. M. Principles of Instrumental Analysis. *Studies in Conservation* **1973**, *18*, 45−47.

(26) Young, V.; Dean, John A.; Merritt, Lynne L.; Settle, Frank A.; Willard, Hobart H. Instrumental Methods of Analysis, 7th Edition. *J. Chem. Educ.* **1989**, *66*, 1 DOI: 10.1021/ed066pa46.2.

(27) Drebushchak, V. A. The Peltier effect. *J. Therm Anal Calorim* **2008**, *91*, 311−315.

(28) Disalvo, F. J. Thermoelectric cooling and power generation. *Science* **1999**, *285* (1979), 703−6.
(29) Carey, P. R. *Biochemical Applications of Raman and Resonance Raman Spectroscopes*; Academic Press, 1982, DOI: 10.1016/b978-0-12-159650-7.x5001-9.
(30) Palonpon, A. F.; Sodeoka, M.; Fujita, K. Molecular imaging of live cells by Raman microscopy. *Curr. Opin Chem. Biol.* **2013**, *17*, 708−15.
(31) Uzunbajakava, N.; Lenferink, A.; Kraan, Y.; Volokhina, E.; Vrensen, G.; Greve, J.; et al. Nonresonant confocal Raman imaging of DNA and protein distribution in apoptotic cells. *Biophys. J.* **2003**, *84*, 3968−3981.
(32) Huang, Y. S.; Karashima, T.; Yamamoto, M.; Hamaguchi, H. O. Molecular-level investigation of the structure, transformation, and bioactivity of single living fission yeast cells by time- and space-resolved Raman spectroscopy. *Biochemistry* **2005**, *44*, 10009−10019.
(33) Wen, C. I.; Hiramatsu, H. The 532-nm-excited hyper-Raman spectroscopy of globular protein and aromatic amino acids. *J. Raman Spectrosc.* **2020**, *51*, 274−278.
(34) Hellerer, T.; Axäng, C.; Brackmann, C.; Hillertz, P.; Pilon, M.; Enejder, A. Monitoring of lipid storage in Caenorhabditis elegans using coherent anti-Stokes Raman scattering (CARS) microscopy. *Proc. Natl. Acad. Sci. U. S. A.* **2007**, *104*, 14658−63.
(35) Nahmad-Rohen, A.; Regan, D.; Masia, F.; McPhee, C.; Pope, I.; Langbein, W.; et al. Quantitative Label-Free Imaging of Lipid Domains in Single Bilayers by Hyperspectral Coherent Raman Scattering. *Anal. Chem.* **2020**, *92*, 14657−14666.
(36) Wu, Y. M.; Chen, H. C.; Chang, W. T.; Jhan, J. W.; Lin, H. L.; Liau, I. Quantitative assessment of hepatic fat of intact liver tissues with coherent anti-stokes Raman scattering microscopy. *Anal. Chem.* **2009**, *81*, 1496−1504.
(37) Evans, C. L.; Xu, X.; Kesari, S.; Xie, X. S.; Wong, S. T. C.; Young, G. S. Chemically-selective imaging of brain structures with CARS microscopy. *Opt Express* **2007**, *15*, 12076−12087.
(38) Evans, C. L.; Potma, E. O.; Puoris'haag, M.; Côté, D.; Lin, C. P.; Xie, X. S. Chemical imaging of tissue in vivo with video-rate coherent anti-Stokes Raman scattering microscopy. *Proc. Natl. Acad. Sci. U. S. A.* **2005**, *102*, 16807−12.
(39) Patel, I. I.; Trevisan, J.; Evans, G.; Llabjani, V.; Martin-Hirsch, P. L.; Stringfellow, H. F.; et al. High contrast images of uterine tissue derived using Raman microspectroscopy with the empty modelling approach of multivariate curve resolution-alternating least squares. *Analyst* **2011**, *136*, 4950−4959.
(40) Vrabie, V.; Gobinet, C.; Piot, O.; Tfayli, A.; Bernard, P.; Huez, R.; et al. Independent component analysis of Raman spectra: Application on paraffin-embedded skin biopsies. *Biomed Signal Process Control* **2007**, *2*, 40−50.
(41) Fu, D.; Lu, F. K.; Zhang, X.; Freudiger, C.; Pernik, D. R.; Holtom, G.; et al. Quantitative chemical imaging with multiplex stimulated Raman scattering microscopy. *J. Am. Chem. Soc.* **2012**, *134*, 3623−6.
(42) Ozeki, Y.; Umemura, W.; Otsuka, Y.; Satoh, S.; Hashimoto, H.; Sumimura, K.; et al. High-speed molecular spectral imaging of tissue with stimulated Raman scattering. *Nat. Photonics* **2012**, *6*, 845−851.
(43) Ando, M.; Hamaguchi, H. Molecular component distribution imaging of living cells by multivariate curve resolution analysis of space-resolved Raman spectra. *J. Biomed Opt* **2014**, *19*, 011016.
(44) Camp, C. H.; Lee, Y. J.; Heddleston, J. M.; Hartshorn, C. M.; Walker, A. R. H.; Rich, J. N.; et al. High-speed coherent Raman fingerprint imaging of biological tissues. *Nat. Photonics* **2014**, *8*, 627−634.
(45) Bratchenko, L. A.; Bratchenko, I. A.; Lykina, A. A.; Komarova, M. V.; Artemyev, D. N.; Myakinin, O. O.; et al. Comparative study of multivariative analysis methods of blood Raman spectra classification. *J. Raman Spectrosc.* **2020**, *51*, 279−92.
(46) Auner, G. W.; Koya, S. K.; Huang, C.; Broadbent, B.; Trexler, M.; Auner, Z.; et al. Applications of Raman spectroscopy in cancer diagnosis. *Cancer and Metastasis Reviews* **2018**, *37*, 691−717.
(47) Hubbard, T. J. E.; Shore, A.; Stone, N. Raman spectroscopy for rapid intra-operative margin analysis of surgically excised tumour specimens. *Analyst* **2019**, *144*, 6479−96.
(48) Jermyn, M.; Mok, K.; Mercier, J.; Desroches, J.; Pichette, J.; Saint-Arnaud, K.; et al. Intraoperative brain cancer detection with Raman spectroscopy in humans. *Sci. Transl Med.* **2015**, *7*, No. 274ra19.
(49) Ichimura, T.; Chiu, L.; Fujita, K.; Kawata, S.; Watanabe, T. M.; Yanagida, T.; et al. Visualizing Cell State Transition Using Raman Spectroscopy. *PLoS One* **2014**, *9*, No. e84478.
(50) Ghita, A.; Pascut, F. C.; Sottile, V.; Denning, C.; Notingher, I. Applications of Raman micro-spectroscopy to stem cell technology: label-free molecular discrimination and monitoring cell differentiation. *EPJ. Tech Instrum* **2015**, *2*, 6.
(51) Germond, A.; Panina, Y.; Shiga, M.; Niioka, H.; Watanabe, T. M. Following Embryonic Stem Cells, Their Differentiated Progeny, and Cell-State Changes During iPS Reprogramming by Raman Spectroscopy. *Anal. Chem.* **2020**, *92*, 14915−23.
(52) Hsu, C.-C.; Xu, J.; Brinkhof, B.; Wang, H.; Cui, Z.; Huang, W. E.; et al. A single-cell Raman-based platform to identify developmental stages of human pluripotent stem cell-derived neurons. *Proc. Natl. Acad. Sci. U. S. A.* **2020**, *117*, 18412−23.
(53) Hashimoto, A.; Yamaguchi, Y.; Chiu, L.; Morimoto, C.; Fujita, K.; Takedachi, M.; et al. Time-lapse Raman imaging of osteoblast differentiation. *Sci. Rep* **2015**, *5*, No. 12529.
(54) Germond, A.; Ichimura, T.; Horinouchi, T.; Fujita, H.; Furusawa, C.; Watanabe, T. M. Raman spectral signature reflects transcriptomic features of antibiotic resistance in Escherichia coli. *Commun. Biol.* **2018**, *1*, 85.
(55) Kobayashi-Kirschvink, K. J.; Nakaoka, H.; Oda, A.; Kamei, K.-i. F.; Nosho, K.; Fukushima, H.; Kanesaki, Y.; Yajima, S.; Masaki, H.; Ohta, K.; Wakamoto, Y. Linear Regression Links Transcriptomic Data and Cellular Raman Spectra. *Cell Syst* **2018**, *7*, 104.
(56) Le Reste, P.; Pilalis, E.; Aubry, M.; McMahon, M.; Cano, L.; Etcheverry, A.; et al. Integration of Raman spectra with transcriptome data in glioblastoma multiforme defines tumour subtypes and predicts patient outcome. *J. Cell Mol. Med.* **2021**, *25*, 10846−56.
(57) Rangan, S.; Schulze, H. G.; Vardaki, M. Z.; Blades, M. W.; Piret, J. M.; Turner, R. F. B. Applications of Raman spectroscopy in the development of cell therapies: State of the art and future perspectives. *Analyst* **2020**, *145*, 2070−2105.
(58) Ichimura, T.; Chiu, L.; Fujita, K.; Machiyama, H.; Yamaguchi, T.; Watanabe, T. M.; et al. Non-label immune cell state prediction using Raman spectroscopy. *Sci. Rep* **2016**, *6*, No. 37562.
(59) Pavillon, N.; Hobro, A. J.; Akira, S.; Smith, N. I. Noninvasive detection of macrophage activation with single-cell resolution through machine learning. *Proc. Natl. Acad. Sci. U. S. A.* **2018**, *115*, E2676−85.
(60) Suzuki, Y.; Kobayashi, K.; Wakisaka, Y.; Deng, D.; Tanaka, S.; Huang, C.-J.; et al. Label-free chemical imaging flow cytometry by high-speed multicolor stimulated Raman scattering. *Proc. Natl. Acad. Sci. U. S. A.* **2019**, *116*, 15842−8.
(61) Huang, K.-C.; Li, J.; Zhang, C.; Tan, Y.; Cheng, J.-X. Multiplex Stimulated Raman Scattering Imaging Cytometry Reveals Lipid-Rich Protrusions in Cancer Cells under Stress Condition. *IScience* **2020**, *23*, No. 100953.
(62) Nitta, N.; Iino, T.; Isozaki, A.; Yamagishi, M.; Kitahama, Y.; Sakuma, S.; et al. Raman image-activated cell sorting. *Nat. Commun.* **2020**, *11*, 3452.
(63) Ouyang, H.; Xu, J.; Zhu, Z.; Long, T.; Yu, C. Rapid discrimination of malignant lesions from normal gastric tissues utilizing Raman spectroscopy system: a meta-analysis. *J. Cancer Res. Clin Oncol* **2015**, *141*, 1835−44.
(64) Shen, A. G.; Ye, Y.; Zhang, J. W.; Wang, X. H.; Hu, J. M.; Xie, W.; et al. Screening of gastric carcinoma cells in the human malignant gastric mucosa by confocal Raman microspectroscopy. *Vib Spectrosc* **2005**, *37*, 225−31.
(65) Hu, Y.; Shen, A.; Jiang, T.; Ai, Y.; Hu, J. Classification of normal and malignant human gastric mucosa tissue with confocal

https://doi.org/10.1021/acsomega.4c00591
ACS Omega 2024, 9, 50049−50063

Raman microspectroscopy and wavelet analysis. *Spectrochim Acta A Mol. Biomol Spectrosc* **2008**, *69*, 378−82.
(66) Garnaik, U. C.; Agarwal, S. A Vibrational Spectroscopic Method for Detection of Rheumatoid Arthritis using Bodily Fluids. *Indian Journal of Pure & Applied Physics* **2023**, *61*, 807−809.
(67) Huang, Z.; Teh, S. K.; Zheng, W.; Mo, J.; Lin, K.; Shao, X.; et al. Integrated Raman spectroscopy and trimodal wide-field imaging techniques for real-time in vivo tissue Raman measurements at endoscopy. *Opt. Lett.* **2009**, *34*, 758−760.
(68) Bratchenko, L. A.; Bratchenko, I. A.; Khristoforova, Y. A.; Artemyev, D. N.; Konovalova, D. Y.; Lebedev, P. A.; Zakharov, V. P. Raman spectroscopy of human skin for kidney failure detection. *J. Biophotonics* **2021**, *14*, e202000360.
(69) Ikeda, H.; Ito, H.; Hikita, M.; Yamaguchi, N.; Uragami, N.; Yokoyama, N.; et al. Raman spectroscopy for the diagnosis of unlabeled and unstained histopathological tissue specimens. *World J. Gastrointest Oncol* **2018**, *10*, 439−48.
(70) Kawabata, T.; Mizuno, T.; Okazaki, S.; Hiramatsu, M.; Setoguchi, T.; Kikuchi, H.; et al. Optical diagnosis of gastric cancer using near-infrared multichannel Raman spectroscopy with a 1064-nm excitation wavelength. *J. Gastroenterol* **2008**, *43*, 283−90.
(71) Zhou, X.; Dai, J.; Chen, Y.; Duan, G.; Liu, Y.; Zhang, H.; et al. Evaluation of the diagnostic potential of ex vivo Raman spectroscopy in gastric cancers: fingerprint versus high wavenumber. *J. Biomed Opt* **2016**, *21*, No. 105002.
(72) Kalyan Kumar, K.; Anand, A.; Chowdary, M. V. P.; Keerthi; Kurien, J.; Murali Krishna, C.; et al. Discrimination of normal and malignant stomach mucosal tissues by Raman spectroscopy: A pilot study. *Vib Spectrosc* **2007**, *44*, 382−7.
(73) Teh, S. K.; Zheng, W.; Ho, K. Y.; Teh, M.; Yeoh, K. G.; Huang, Z. Diagnosis of gastric cancer using near-infrared Raman spectroscopy and classification and regression tree techniques. *J. Biomed Opt* **2008**, *13*, No. 034013.
(74) Teh, S. K.; Zheng, W.; Ho, K. Y.; Teh, M.; Yeoh, K. G.; Huang, Z. Diagnostic potential of near-infrared Raman spectroscopy in the stomach: differentiating dysplasia from normal tissue. *Br. J. Cancer* **2008**, *98*, 457−65.
(75) Bergholt, M. S.; Zheng, W.; Lin, K.; Ho, K. Y.; Teh, M.; Yeoh, K. G.; et al. Characterizing variability in in vivo Raman spectra of different anatomical locations in the upper gastrointestinal tract toward cancer detection. *J. Biomed Opt* **2011**, *16*, No. 037003.
(76) Haka, A. S.; Volynskaya, Z.; Gardecki, J. A.; Nazemi, J.; Shenk, R.; Wang, N.; et al. Diagnosing breast cancer using Raman spectroscopy: prospective analysis. *J. Biomed Opt* **2009**, *14*, No. 054023.
(77) Kamemoto, L. E.; Misra, A. K.; Sharma, S. K.; Goodman, M. T.; Luk, H.; Dykes, A. C.; et al. Near-Infrared Micro-Raman Spectroscopy for *in Vitro* Detection of Cervical Cancer. *Appl. Spectrosc.* **2010**, *64*, 255−61.
(78) Ramos, I. R. M.; Malkin, A.; Lyng, F. M. Current Advances in the Application of Raman Spectroscopy for Molecular Diagnosis of Cervical Cancer. *Biomed Res. Int.* **2015**, *2015*, 1−9.
(79) Wills, H.; Kast, R.; Stewart, C.; Rabah, R.; Pandya, A.; Poulik, J.; et al. Raman spectroscopy detects and distinguishes neuroblastoma and related tissues in fresh and (banked) frozen specimens. *J. Pediatr Surg* **2009**, *44*, 386−91.
(80) Lin, K.; Wang, J.; Zheng, W.; Ho, K. Y.; Teh, M.; Yeoh, K. G.; et al. Rapid Fiber-optic Raman Spectroscopy for Real-Time *In Vivo* Detection of Gastric Intestinal Metaplasia during Clinical Gastroscopy. *Cancer Prevention Research* **2016**, *9*, 476−83.
(81) Chen, H.; Li, X.; Broderick, N. G. R.; Xu, W. Low-resolution fiber-optic Raman spectroscopy for bladder cancer diagnosis: A comparison study of varying laser power, integration time, and classification methods. *J. Raman Spectrosc.* **2020**, *51*, 323−34.
(82) Chen, Y.; Dai, J.; Zhou, X.; Liu, Y.; Zhang, W.; Peng, G. Raman spectroscopy analysis of the biochemical characteristics of molecules associated with the malignant transformation of gastric mucosa. *PLoS One* **2014**, *9*, e93906.
(83) Teh, S. K.; Zheng, W.; Ho, K. Y.; Teh, M.; Yeoh, K. G.; Huang, Z. Near-infrared Raman spectroscopy for early diagnosis and typing of adenocarcinoma in the stomach. *British Journal of Surgery* **2010**, *97*, 550−7.
(84) Yao, H.; Tao, Z.; Ai, M.; Peng, L.; Wang, G.; He, B.; et al. Raman spectroscopic analysis of apoptosis of single human gastric cancer cells. *Vib Spectrosc* **2009**, *50*, 193−197.
(85) Boardman, A. K.; Wong, W. S.; Premasiri, W. R.; Ziegler, L. D.; Lee, J. C.; Miljkovic, M.; et al. Rapid detection of bacteria from blood with surface-enhanced Raman spectroscopy. *Anal. Chem.* **2016**, *88*, 8026−8035.
(86) Wei, D.; Chen, S.; Liu, Q. Review of Fluorescence Suppression Techniques in Raman Spectroscopy. *Appl. Spectrosc Rev.* **2015**, *50*, 387−406.
(87) Eberhardt, K.; Stiebing, C.; Matthäus, C.; Schmitt, M.; Popp, J. Advantages and limitations of Raman spectroscopy for molecular diagnostics: an update. *Expert Rev. Mol. Diagn* **2015**, *15*, 773−87.
(88) Ashton, L.; Lau, K.; Winder, C. L.; Goodacre, R. Raman Spectroscopy: Lighting up the Future of Microbial Identification. *Future Microbiol* **2011**, *6*, 991−7.
(89) Lorenz, B.; Wichmann, C.; Stöckel, S.; Rösch, P.; Popp, J. Cultivation-Free Raman Spectroscopic Investigations of Bacteria. *Trends Microbiol* **2017**, *25*, 413−24.
(90) Strola, S. A.; Baritaux, J.-C.; Schultz, E.; Simon, A. C.; Allier, C.; Espagnon, I.; et al. Single bacteria identification by Raman spectroscopy. *J. Biomed Opt* **2014**, *19*, No. 111610.
(91) Smith, R.; Wright, K. L.; Ashton, L. Raman spectroscopy: an evolving technique for live cell studies. *Analyst* **2016**, *141*, 3590−600.
(92) de Siqueira e Oliveira, F. S.; da Silva, A. M.; Pacheco, M. T. T.; Giana, H. E.; Silveira, L. Biochemical characterization of pathogenic bacterial species using Raman spectroscopy and discrimination model based on selected spectral features. *Lasers Med. Sci.* **2021**, *36*, 289−302.
(93) Kunstar, A.; Leferink, A. M.; Okagbare, P. I.; Morris, M. D.; Roessler, B. J.; Otto, C.; et al. Label-free Raman monitoring of extracellular matrix formation in three-dimensional polymeric scaffolds. *J. R Soc. Interface* **2013**, *10*, No. 20130464.
(94) Khmaladze, A.; Kuo, S.; Kim, R. Y.; Matthews, R. V.; Marcelo, C. L.; Feinberg, S. E.; et al. Human Oral Mucosa Tissue-Engineered Constructs Monitored by Raman Fiber-Optic Probe. *Tissue Eng. Part C Methods* **2015**, *21*, 46−51.
(95) Gentleman, E.; Swain, R. J.; Evans, N. D.; Boonrungsiman, S.; Jell, G.; Ball, M. D.; et al. Comparative materials differences revealed in engineered bone as a function of cell-specific differentiation. *Nat. Mater.* **2009**, *8*, 763−770.
(96) Bergholt, M. S.; St-Pierre, J.-P.; Offeddu, G. S.; Parmar, P. A.; Albro, M. B.; Puetzer, J. L.; et al. Raman Spectroscopy Reveals New Insights into the Zonal Organization of Native and Tissue-Engineered Articular Cartilage. *ACS Cent Sci.* **2016**, *2*, 885−95.
(97) Goodell, M. A.; Nguyen, H.; Shroyer, N. Somatic stem cell heterogeneity: diversity in the blood, skin and intestinal stem cell compartments. *Nat. Rev. Mol. Cell Biol.* **2015**, *16*, 299−309.
(98) Downes, A.; Mouras, R.; Bagnaninchi, P.; Elfick, A. Raman spectroscopy and CARS microscopy of stem cells and their derivatives. *J. Raman Spectrosc.* **2011**, *42*, 1864−70.
(99) Hentze, H.; Soong, P. L.; Wang, S. T.; Phillips, B. W.; Putti, T. C.; Dunn, N. R. Teratoma formation by human embryonic stem cells: Evaluation of essential parameters for future safety studies. *Stem Cell Res.* **2009**, *2*, 198−210.
(100) Nagano, K.; Yoshida, Y.; Isobe, T. Cell surface biomarkers of embryonic stem cells. *Proteomics* **2008**, *8*, 4025−35.
(101) Chan, J. W.; Lieu, D. K.; Huser, T.; Li, R. A. Label-Free Separation of Human Embryonic Stem Cells and Their Cardiac Derivatives Using Raman Spectroscopy. *Anal. Chem.* **2009**, *81*, 1324−31.
(102) Tan, Y.; Konorov, S. O.; Schulze, H. G.; Piret, J. M.; Blades, M. W.; Turner, R. F. B. Comparative study using Raman microspectroscopy reveals spectral signatures of human induced pluripotent cells more closely resemble those from human embryonic

https://doi.org/10.1021/acsomega.4c00591
ACS Omega 2024, 9, 50049−50063

stem cells than those from differentiated cells. *Analyst* **2012**, *137*, 4509−4515.
(103) Swain, R. J.; Kemp, S. J.; Goldstraw, P.; Tetley, T. D.; Stevens, M. M. Assessment of Cell Line Models of Primary Human Cells by Raman Spectral Phenotyping. *Biophys. J.* **2010**, *98*, 1703−11.
(104) Verrier, S.; Zoladek, A.; Notingher, I. Raman Micro-Spectroscopy as a Non-invasive Cell Viability Test. *Methods Mol. Biol.* **2011**, *740*, 179−89.
(105) Verrier, S.; Notingher, I.; Polak, J. M.; Hench, L. L. In situ monitoring of cell death using Raman microspectroscopy. *Biopolymers* **2004**, *74*, 157−62.
(106) Notingher, I.; Verrier, S.; Haque, S.; Polak, J. M.; Hench, L. L. Spectroscopic study of human lung epithelial cells (A549) in culture: Living cells versus dead cells. *Biopolymers* **2003**, *72*, 230−40.
(107) Han, X. X.; Rodriguez, R. S.; Haynes, C. L.; Ozaki, Y.; Zhao, B. Surface-enhanced Raman spectroscopy. *Nature Reviews Methods Primers 2022 1:1* **2021**, *1* (87), 1−17.
(108) Matousek, P.; Stone, N. Recent advances in the development of Raman spectroscopy for deep non-invasive medical diagnosis. *J. Biophotonics* **2013**, *6*, 7−19.
(109) Cheng, X.; Liang, H.; Li, Q.; Wang, J.; Liu, J.; Zhang, Y.; et al. Raman spectroscopy differ leukemic cells from their healthy counterparts and screen biomarkers in acute leukemia. *Spectrochim Acta A Mol. Biomol Spectrosc* **2022**, *281*, No. 121558.
(110) Alattar, N.; Daud, H.; Al-Majmaie, R.; Zeulla, D.; Al-Rubeai, M.; Rice, J. H. Surface-enhanced Raman scattering for rapid hematopoietic stem cell differentiation analysis. *Appl. Opt.* **2018**, *57*, E184−E189.
(111) Agrawal, G.; Samal, S. K. Raman Spectroscopy for Advanced Polymeric Biomaterials. *ACS Biomater Sci. Eng.* **2018**, *4*, 1285−99.
(112) Fleischmann, M.; Hendra, P. J.; McQuillan, A. J. Raman spectra of pyridine adsorbed at a silver electrode. *Chem. Phys. Lett.* **1974**, *26*, 163−166.
(113) Jeanmaire, D. L.; Van Duyne, R. P. Surface raman spectroelectrochemistry. *J. Electroanal Chem. Interfacial Electrochem* **1977**, *84*, 1−20.
(114) Langer, J.; Jimenez de Aberasturi, D.; Aizpurua, J.; Alvarez-Puebla, R. A.; Auguié, B.; Baumberg, J. J.; et al. Present and Future of Surface-Enhanced Raman Scattering. *ACS Nano* **2020**, *14*, 28−117.
(115) Cialla-May, D.; Krafft, C.; Rösch, P.; Deckert-Gaudig, T.; Frosch, T.; Jahn, I. J.; et al. Raman Spectroscopy and Imaging in Bioanalytics. *Anal. Chem.* **2022**, *94*, 86−119.
(116) Laing, S.; Gracie, K.; Faulds, K. Multiplex in vitro detection using SERS. *Chem. Soc. Rev.* **2016**, *45*, 1901−18.
(117) Lane, L. A.; Qian, X.; Nie, S. SERS Nanoparticles in Medicine: From Label-Free Detection to Spectroscopic Tagging. *Chem. Rev.* **2015**, *115*, 10489−529.
(118) Habuchi, S.; Cotlet, M.; Gronheid, R.; Dirix, G.; Michiels, J.; Vanderleyden, J.; et al. Single-molecule surface enhanced resonance Raman spectroscopy of the enhanced green fluorescent protein. *J. Am. Chem. Soc.* **2003**, *125*, 8446−8447.
(119) Lu, G.; De Keersmaecker, H.; Su, L.; Kenens, B.; Rocha, S.; Fron, E.; et al. Live-cell SERS endoscopy using plasmonic nanowire waveguides. *Adv. Mater.* **2014**, *26*, 5124−8.
(120) Bergholt, M. S.; Serio, A.; McKenzie, J. S.; Boyd, A.; Soares, R. F.; Tillner, J.; et al. Correlated Heterospectral Lipidomics for Biomolecular Profiling of Remyelination in Multiple Sclerosis. *ACS Cent Sci.* **2018**, *4*, 39−51.
(121) Tfayli, A.; Gobinet, C.; Vrabie, V.; Huez, R.; Manfait, M.; Piot, O. Digital dewaxing of Raman signals: Discrimination between nevi and melanoma spectra obtained from paraffin-embedded skin biopsies. *Appl. Spectrosc.* **2009**, *63*, 564−570.
(122) Gaifulina, R.; Maher, A. T.; Kendall, C.; Nelson, J.; Rodriguez-Justo, M.; Lau, K.; et al. Label-free Raman spectroscopic imaging to extract morphological and chemical information from a formalin-fixed, paraffin-embedded rat colon tissue section. *Int. J. Exp Pathol* **2016**, *97*, 337−50.
(123) Huang, Z.; McWilliams, A.; Lam, S.; English, J.; McLean, D.; Lui, H.; et al. Effect of formalin fixation on the near-infrared Raman spectroscopy of normal and cancerous human bronchial tissues. *Int. J. Oncol.* **2003**, *23* (3), 649−655.
(124) Meade, A. D.; Clarke, C.; Draux, F.; Sockalingum, G. D.; Manfait, M.; Lyng, F. M.; et al. Studies of chemical fixation effects in human cell lines using Raman microspectroscopy. *Anal Bioanal Chem.* **2010**, *396*, 1781−91.
(125) Kallepitis, C.; Bergholt, M. S.; Mazo, M. M.; Leonardo, V.; Skaalure, S. C.; Maynard, S. A.; et al. Quantitative volumetric Raman imaging of three dimensional cell cultures. *Nat. Commun.* **2017**, *8*, No. 14843.
(126) Lieber, C. A.; Mahadevan-Jansen, A. Automated Method for Subtraction of Fluorescence from Biological Raman Spectra. *Appl. Spectrosc.* **2003**, *57*, 1363−7.
(127) Zhao, J.; Lui, H.; McLean, D. I.; Zeng, H. Automated Autofluorescence Background Subtraction Algorithm for Biomedical Raman Spectroscopy. *Appl. Spectrosc.* **2007**, *61*, 1225−32.
(128) Hedegaard, M. A. B.; Bergholt, M. S.; Stevens, M. M. Quantitative multi-image analysis for biomedical Raman spectroscopic imaging. *J. Biophotonics* **2016**, *9*, 542−50.
(129) Fortuni, B.; Ricci, M.; Vitale, R.; Inose, T.; Zhang, Q.; Hutchison, J. A.; et al. SERS Endoscopy for Monitoring Intracellular Drug Dynamics. *ACS Sens* **2023**, *8*, 2340−2347.
(130) Dasari, S.; Singh, S.; Abbas, Z.; Sivakumar, S.; Patra, A. K. Luminescent lanthanide(III) complexes of DTPA-bis(amido-phenyl-terpyridine) for bioimaging and phototherapeutic applications. *Spectrochim Acta A Mol. Biomol Spectrosc* **2021**, *256*, No. 119709.
(131) Fuentes, A. M.; Narayan, A.; Milligan, K.; Lum, J. J.; Brolo, A. G.; Andrews, J. L.; et al. Raman spectroscopy and convolutional neural networks for monitoring biochemical radiation response in breast tumour xenografts. *Sci. Rep* **2023**, *13*, 1530.

https://doi.org/10.1021/acsomega.4c00591
ACS Omega 2024, 9, 50049−50063